Position Estimation via Accelerometer Data

Introduction

Inertial sensors belong to a class of sensors that offer high precision indications of changes in kinematic state over short time periods. Other systems like GPS and GSM triangulation can offer relatively high accuracy in position but do not have high precision. Measurements of changes in the inertial frame of micro-mechanically machined capacitive sensors can be used to infer changes in position and in conjunction with the other location mechanisms can be used to achieve a highly precise and accuracy location mechanism. The application of numerical integration and gravity filtering techniques are critical to leveraging the inertial sensors accuracy. Using a sensor platform to record acceleration and angular rate, this lab will investigate the effects on filtering and sample rate on position estimates inferred from the inertial measurements.

Initial Tests

The main obstacle for obtaining position estimates from acceleration data is removing the effects of integration drift. Small bias in the acceleration data double-integrates large changes in position, even for stationary sensors. An obvious bias is gravity, which acts -9.81$\frac{m}{s^2}$ constantly in the z-direction. Other biases include zero-mean signal noise in the acceleration data which develop a non-zero bias when digitally sampled. Several three dimensional test were performed in which the gravitational bias and initial orientation of the sensors with respect to gravity was found in a calibration period. The gyro and accelerometer measurements were then fused utilizing a rotation matrix to find the acceleration in gravities reverence frame. It was found that small errors in the estimate of the orientation caused by drift in the gyro resulted in large nonlinear drift in the acceleration due to the estimated orientation of the sensors being misaligned with gravity. This misalignment caused components of the gravity offset to be subtracted from the wrong axes resulting in steady state error in the perceived acceleration. Once this error was integrated twice large errors in position an order of magnitude large than actual movement were observed.

Experimental Setup

Since bias error corrupts the acceleration data, a repeatable experiment is implemented in order to analyze the errors and statistically predict which sampling frequencies and low-pass filtering produce the most accurate data. Our repeatable setup explores prediction accuracy with one dimensional stepped constant acceleration.

TABLE 1: EXPERIMENTAL FACTOR LEVELS

Factors	Low-pass filter cutoff	Sampling Rate
Level 1	20 Hz	500 Hz
Level 2	10 Hz	250 Hz
Level 3	Infinite	125 Hz

A linear rail isolates motion of the sensor to a single axis, see Figure 5. A low-friction cart, with the sensor clamped onto it, accelerates constantly by a falling bolt which is tethered to the cart by a string. The track is slightly inclined so there is a period of constant acceleration while the bolt falls and another period of constant acceleration in the opposite direction after the bolt hits the ground, see Figure 6. Before each trial, the cart is left still to record calibration data of the components of gravity present in each sensor axis. The sensor platform logs the values to delimited file via a serial connection. The experiment has two factors: hardware low-pass filter cutoff frequency and sampling frequency with three levels each as seen in Table 1. Each treatment application is randomly applied in order to minimize a consistent effects from uncontrollable factors.

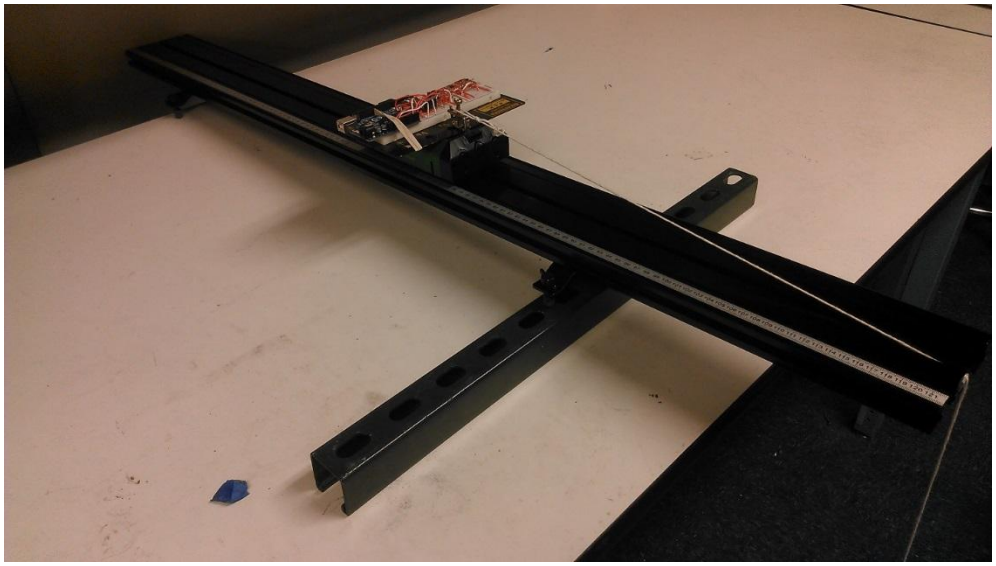

FIGURE 1: LINEAR RAIL EXPERIMENTAL SETUP

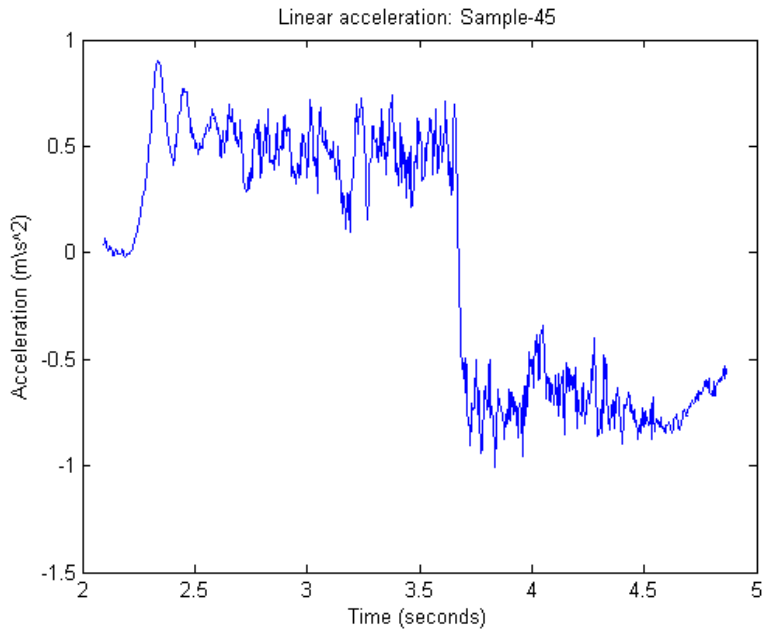

FIGURE 2: SAMPLED CONSTANT ACCELERATION AND DECELERATION

Materials

MMA8452Q 3-Axis Accelerometer	Arduino Uno
Breadboard and Wiring	Weight
Low-Friction Track (120cm)	Twine
Low-Friction Cart	Matlab
Clamp	Temperature sensor

Trial Procedure

A sensor board is constructed with a MMA8452Q 3-Axis accelerometer on an I2C bus connected to an 8 bit Atmel 328 microcontroller. Data is relayed from the sensor to a computer via a USART serial connection and stored in a csv format with each accelerometer axis as produced by the on board analog to digital converter and the time recorded between samples in microseconds. The cart is first placed on an inclined track and the sensor board is clamped down to the cart. The initial temperature is recorded and the position of the front of the cart is measured from the linear scale on the track to +/-.5mm. Acceleration of the cart is achieved by attaching a string between the cart and a weight. When the weight is dropped it would overcome gravity and accelerate until it hit the ground ending the forward acceleration step. Then gravitational acceleration would cause a step of negative acceleration for the remainder of the test. A piece of paper folded into a triangle is placed 3 centimeters before the predicted end point along the scale as seen in Figure 8. The cart would hit this triangle and push it up to the maximum distance, from which the actual maximum distance traveled could be found to a precision of +/-.5mm. For each test a small calibration is performed with a three second delay, then the weight is moved near to the point where it would start supporting the weight of the cart and dropped. When the cart has reached its maximum distance traveled it is allowed to slide back for a second before being caught and ending data collection.

The treatments are applied randomly based on ordered numbers generated by a computer pseudo random number generator in Matlab. At the end of the test the temperature is measured again.

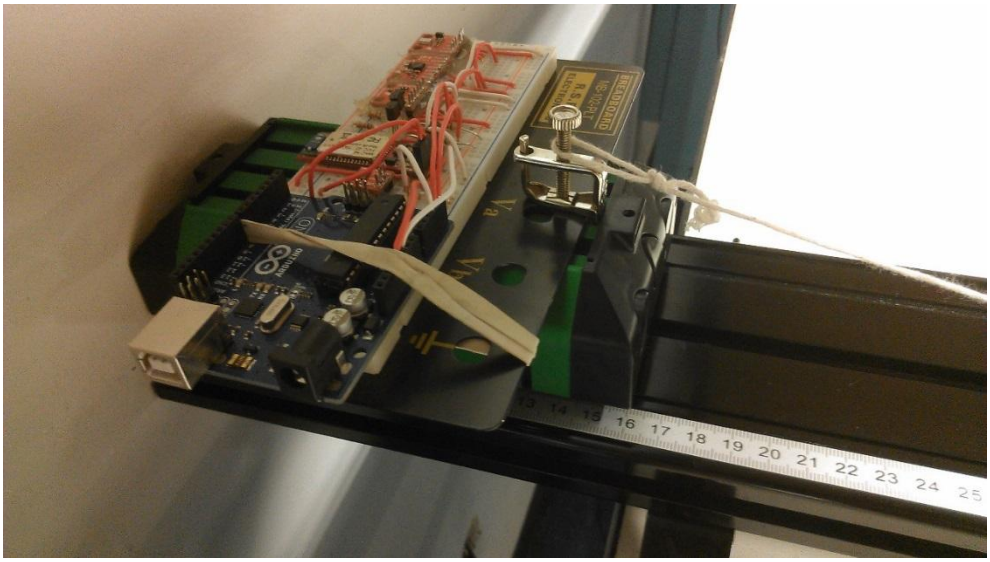

Figure 3: Acceleration Module Setup

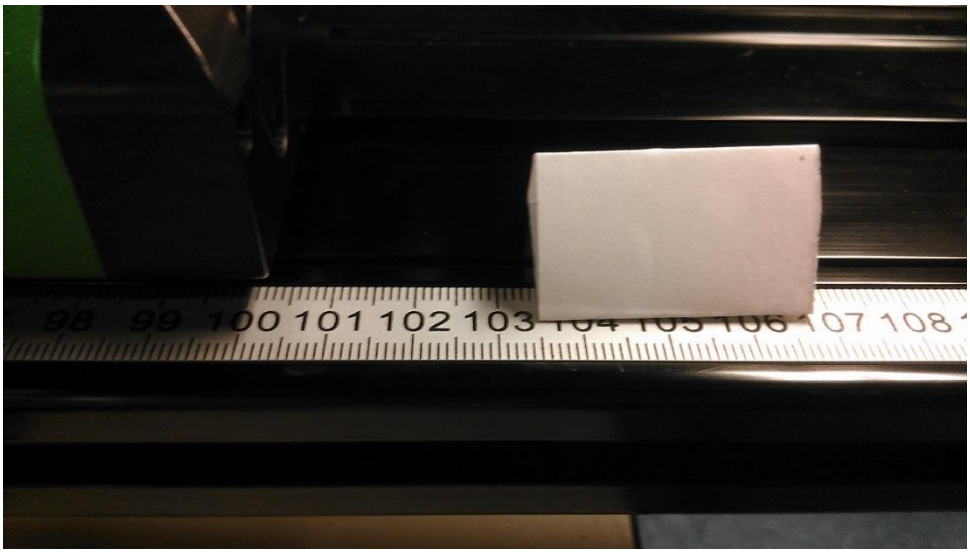

Figure 4: Cart Apex of Travel

Analysis

The data is imported into a numerical analysis program and integrated with time using the trapezoidal method in order to estimated velocity, the velocity is again integrated to estimate the change position. The force of gravity is determined from the calibration data at the beginning of each sample by taking the sum of the squares of the component in each axis defined by the mean of each axis results during the calibration period and dividing by the true gravitation constant. The components of gravity and sensor bias are removed by subtracting the mean values recorded during the calibration period from each axis. The

start and end times of the data are numerically determined from the beginning and end of positive velocity in a first pass estimate and buffered on each side with a constant additional time. The acceleration data is then reintegrated over these times to reduce drift errors due to inconsistent delays before release. The resulting velocity data is seen in Figure 9.

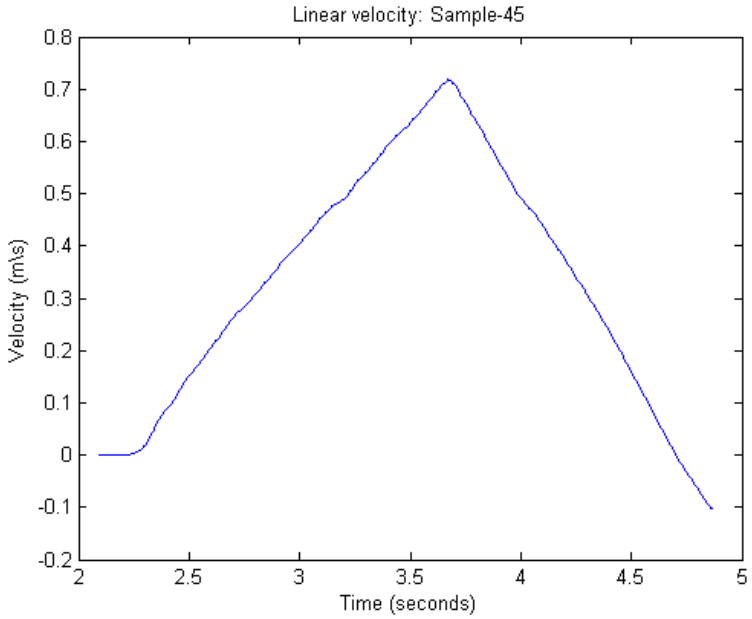

FIGURE 5: ESTIMATED VELOCITY

The position is extracted from this data by finding the maximum estimated distance reached. Using this data and the measured true distances traveled the relative errors are then computed. The relative errors are then tested for normality, equality of variance, and equality of means within Matlab.

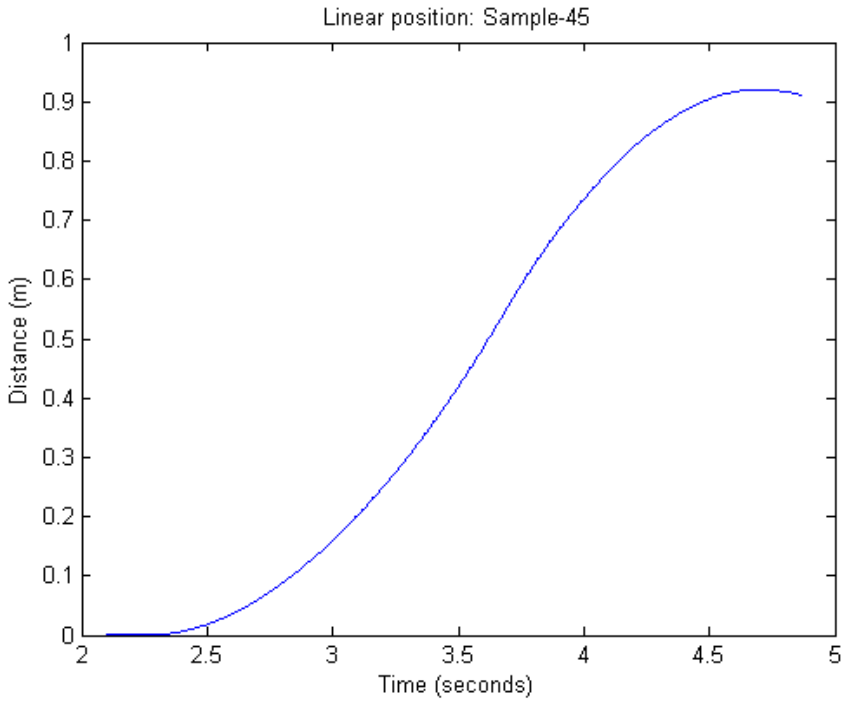

FIGURE 6: ESTIMATED POSITION

Error

The measured error of this experiment derives from the difference between the estimated and actual maximum distance travelled, normalized by the actual distance travelled.

$$error = \frac{|distance_{estimated} - distance_{measured}|}{distance_{measured}}$$

The measured error is calculated using estimated difference determined between the start and maximum estimated position and subtracted from the true distance traveled and then divided by the true distance traveled to arrive at the relative error.

The main quantifiable sources of error occurs as products of the experimental setup and sensors limitations. The experimental setup errors includes uncertainty in the alignment of the accelerometer axis with the axis of motion, error in keeping the alignment constant after the calibration and error in the measurement of actual distance traveled. The sources of error in the sensor measurements include error due to temperature change, discretion error, and sensor error due to inaccuracies in the MEM sensors and amplifiers due to non-linearity, electrical noise, and sensor sensitivity. The sensor measurement errors have to be integrated over all time with the mean acceleration and sampling period in order to find their effect. Also the integration errors depend on an uncertainty in the sampling period and their rate of change with respect to this uncertainty must also take into account. The sum of the squares of all of these error produce the theoretical uncertainty of the experiment as shown in the equations below.

The average magnitude in acceleration is about $a_{output} = .75\frac{m}{s^2}$, the average sampling rate is dependent on the sampling rate applied to the treatment. The average value of gravity is taken at to be $G = 9.81\ m/s^2$, the number of bits in the DAC is $n = 10$. The sampling rate report time is recorded in microseconds based on the time between the start of sensor request times with a resolution of a microseconds producing an $f_{sampling} = 10^6\ Hz$. The alignment error in the track affecting calibration is measured to be about $\alpha_{track} = 2\%$. The alignment of the sensor on the cart is estimated at $\alpha_{cart} = 3\%$. The temperature at the start of the test is 23.5 C and the temperature at the end of the test is taken at 22.0 C. The uncertainty in the measurement of the scale is half the size of the scale divisions $u_{scale} = .5\ mm$. The resulting theoretical uncertainty at the maximum sampling rate is approximately 10 cm. Because the measured values are within a factor of 2 of the theoretical uncertainties, it is reasonable to conclude that there were no other factors that caused effects in the result. It is reasonable to assume that in reality a large portion of this error would cancel out where as the theoretical estimate assumes it is at its maximum value.

$$u_{total} = \sqrt{u_{integration}^2 + \left(\frac{d(u_{integration})}{dt} u_{rate}\right)^2 + u_{measured}^2}$$

$$u_{integration} = \frac{1}{2}\sqrt{u_{sensor}^2 + u_{discretion}^2 + u_{temperature}^2 + u_{misaligment}^2}\, dt_{average}\Delta t$$

$$u_{sensor} = u_{sensitivity} + u_{electrical} + u_{linearity} = 2.5\%(X_{output})$$

$$u_{discretion} = \frac{G}{2^n} = \frac{9.8}{1024}$$

$$u_{rate} = \frac{2}{f_{sampling}} = 4\,ms$$

$$u_{temperature} = .008\%(T_{final} - T_{start})$$

$$u_{misalignment} = sin(\alpha_{track} + \alpha_{cart})X_{output}$$

$$u_{measured} = 2(u_{scale}) = 1\,mm$$

The major random source of error affecting the experiment is the initial cart-track alignment. The component of gravity removed during the calibration could be partially reintroduced once the cart began to move and during its path down the track. This error is amplified during the integration showing up as a constant velocity bias. Because the cart could not easily be aligned at the beginning of each test beyond the angles constrained by the track, this parameter could change with each sample. The major constant source of error is the alignment of the sensor with the track path. This alignment is consistent throughout the test due to the fixed nature of the board on the cart.

Results

The results below indicate a consistent negative bias in the mean relative error. This was attributed to imperfect alignment of the sensors with the axis of motion. These components cannot easily be integrated back into the accelerations with an accuracy less than their magnitude due to imperfections of the alignment of the cart on the track. For this reason a second test was not performed taking into account these additional axes. One noticeable pattern in the data is a smaller variation in the data at the maximum sampling rate and larger variation in the reduced sampling rates at 250 Hz and 125 Hz. Observation of these trends was used to design tests for the significance of any effects caused by the two factors.

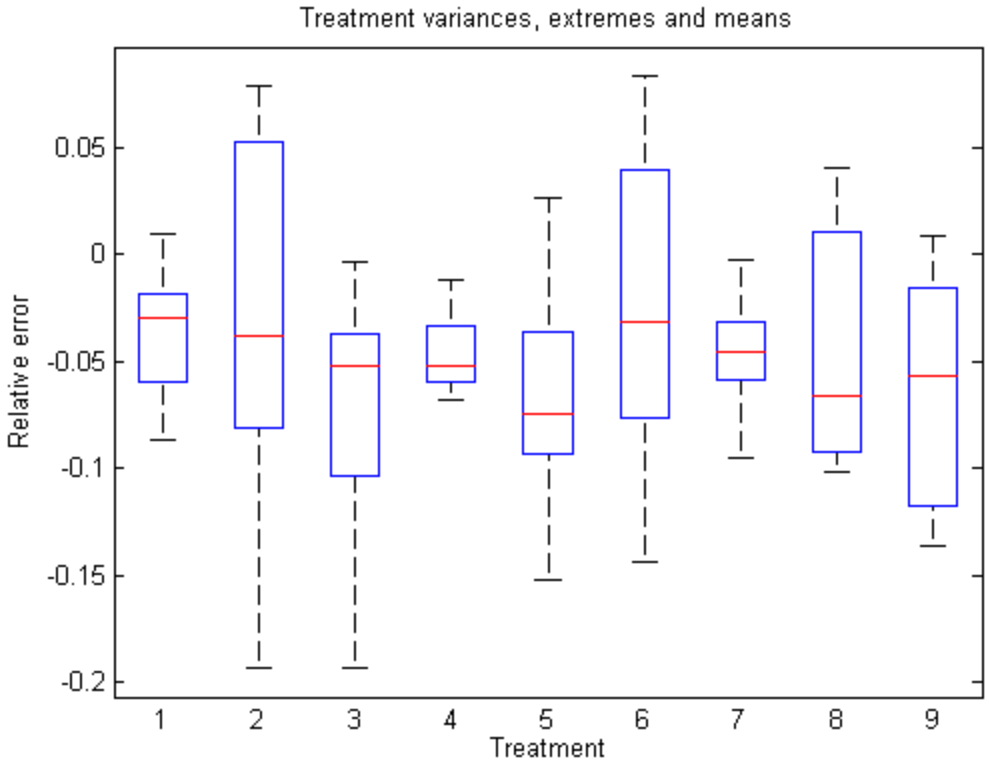

Filter Cutoff	20 Hz Low-Pass			10Hz Low-Pass			No Low-Pass		
Sampling Rate	500Hz	250Hz	125Hz	500Hz	250Hz	125Hz	500Hz	250Hz	125Hz
Treatment	1	2	3	4	5	6	7	8	9
	-2.05	-2.48	-0.35	-6.27	-8.26	-3.32	-3	0.92	-3.54
	-6.58	4.1	-8.61	-6.83	-15.21	0.61	-6.08	-10.14	-12.49
	0.92	7.88	-2.74	-5.63	2.62	-3.38	-3.25	-9.19	0.86
	-5.36	-19.31	-4.96	-5.22	-9.04	-14.43	-4.12	4.01	0.43
	-8.67	-9.13	-12.15	-1.17	-4.48	8.3	-0.25	-4.21	-10.97
	-17.5	-7.19	-19.29	-2.36	-9.59	7.27	-5.66	-9.04	-13.66
	-3.67	6.43	-5.48	-5.29	-6.73	-11.88	-4.95	1.24	-6.58
	-2.21	-5.11	-4.65	-4.38	-2.78	-3.1	-9.54	-9.36	-4.87

Mean Error	-3.67	-3.10	-7.28	-4.64	-6.68	-2.49	-4.61	-4.47	-6.35
95% C.I.	2.50	7.44	4.91	1.59	4.31	6.56	2.21	4.70	4.58

Analysis

The histogram of the relative errors in each treatment indicates good evidence that they come from normally distributed populations. The samples are compared with different bin sizes which revealed a general trend of more frequent occurrences centered near the mean of the sample and less frequent observations occur near the tails. The treatments missing tails on one side can be accepted because they show approximately normally distributed behavior with chance occurrences in the edge bins that do not clearly suggest skewed parent population distributions.

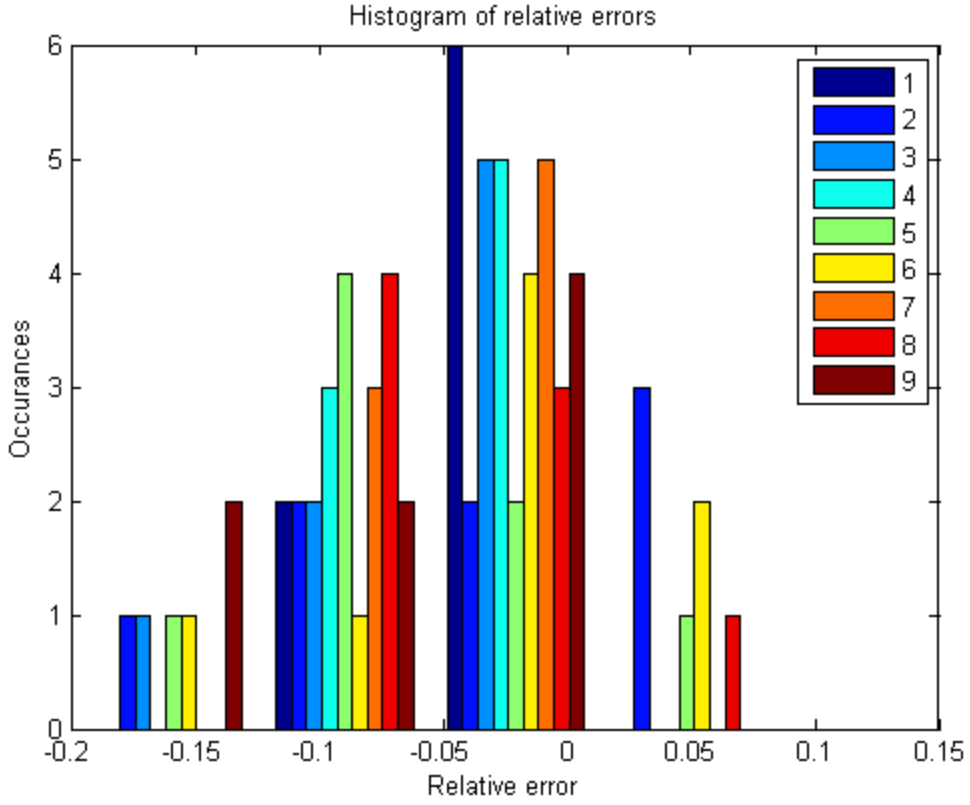

FIGURE 7: HISTOGRAM OF RELATIVE ERROR

From the justification of the normality assumption it is possible to run Bartlett's tests with the hypothesis that the sample of each treatment comes from a normal distribution with the same variance, against the alternative that they come from normal distributions with different variances. P represents the probability of observing the samples taken, or ones more extreme, by chance if the null hypothesis of equal variances is true. Small values of P indicate that there is low probability that the variances could be as observed by chance if they are really the same.

Bartlett's variance test	P-value
All treatments	0.3%
Maximum sampling rate	62.5%
Reduced sampling rate	51.1%

These test results indicate that the variances of all treatments cannot be considered to be equal with 95% confidence. Tests of the samples treated by reducing the sampling rate indicates that the hypothesis that their variances are equal cannot be rejected with greater than 95% confidence. Similarly tests of the samples treated by sampling at the maximum possible rate suggests that the hypothesis that the samples have the same variance should not be rejected.

With the knowledge of the treatments with equal variance tests of the hypothesis that the samples come from normally distributed populations with the same variance and mean can be tested against the alternative hypothesis that they come from normally distributed populations with the same variance but different means. P represents the confidence with which the null hypothesis should not be rejected.

The first test utilized a single factor ANOVA to test for the difference in means for the maximum sampling rate treatments. The levels consisted of the different low-pass filter cutoff frequencies.

Single factor ANOVA	Filter level
P-value	70.5%

The result of this test indicates that the hypothesis that the means of the relative error are unaffected by the low pass filter cannot with greater than 95% confidence. A graphical description of the data used in this test shown below indicates the mean with a red line, the populations maximum extent with a black line, 95% confidence intervals at the intersection of the oblique and vertical blue lines, and the 75% percentile of the data with the horizontal blue lines.

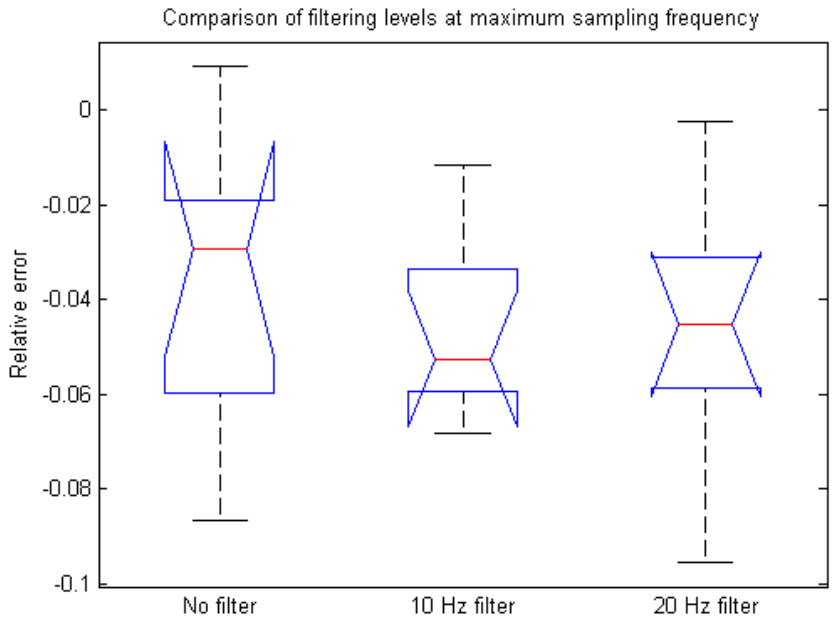

FIGURE 8 : 500 HZ SAMPLES AT VARIOUS FILTERING LEVELS

The second test is formulated as a two way ANOVA test of the hypothesis that the means of the down sampled tests (250 and 125 Hz) come from normally distributed populations with the same variance and mean against the alternate hypothesis that they came from normally distributed populations with equal variance but different means.

Two factor ANOVA	Sampling level	Filter level	Interaction
P-value	75.3%	93.9%	21.0%

This test suggests that there is no reason to reject hypothesis that the means are unaffected by either low-pass filter cutoff frequency or sampling rate for sample rates below the maximum sampling rate. At the sampling level and the filter level there are very high probabilities that the difference in the means could happen by chance, and although the probability that there is an interaction is much lower, it is above the critical level required to say that the hypothesis that there is no effect should be rejected. The data is shown in a separated form in figures 9 and 10 which help reveal why this is the case.

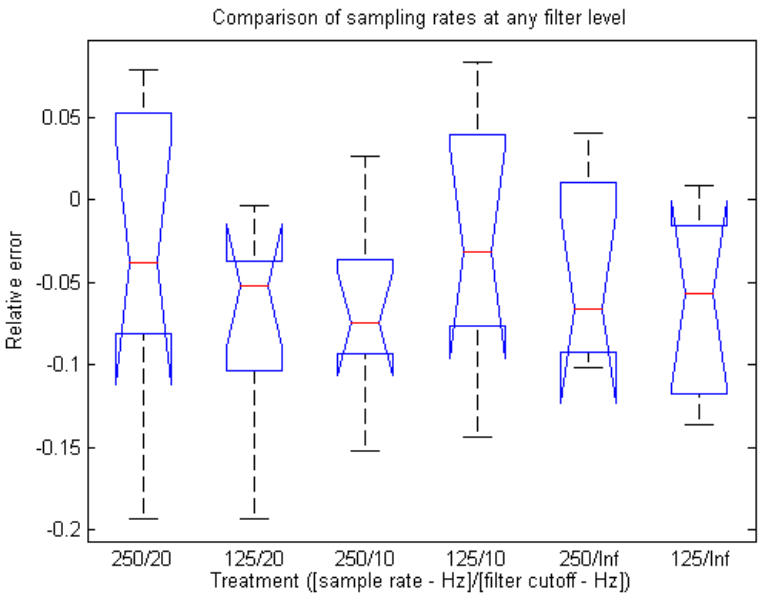

FIGURE 9: EXPERIMENTAL RELATIVE ERROR RESULTS

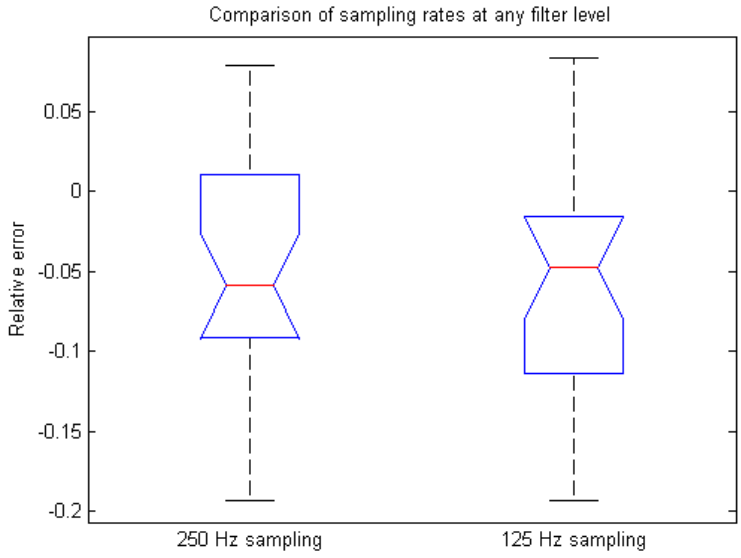

FIGURE 10: COMPARISON OF REDUCED SAMPLING RATE POPULATIONS

The final analysis gains insight from a Welches t-test with the hypothesis that the samples from the maximum sampling rate treatment come from the same normally distributed population as the samples from treatments with the lower sampling rates against the hypothesis that they do not come from normally distributed populations with equal means. This test only relies on the normality assumption and takes into account the different variances and sample sizes of the combined samples.

Welche's t-test	Equal means
P-value	59.1%

The result is that there is little reason to doubt the hypothesis that the means of the 500 Hz samples come from a population with the same mean as the 250 and 125 Hz samples. The conclusion is that neither sampling rate nor filtering cutoff rates have an effect on the mean of the populations.

Conclusions

The data indicates that it is unlikely that there is a difference in the mean relative error in estimated distance as a result of either low pass filtering at various rates or sampling at lower rates under the tested conditions. The analysis suggests that it is possible that there is a significant difference in the variance of the maximum sampling rates and reduced sampling rates although there is not enough evidence to doubt the conclusion that the variance of either of the two reduced sampling rates are different. Considering approximately linear relationship in computational with sampling capability, the results suggest that if the variance of the estimated relative error in position is not important, a slower sampling rate without filtering should be chosen to reduce cost. If a smaller variance in the relative estimated error is required sampling should be performed as quickly as possible without filtering post processing. These suggestions only are valid under the experimental conditions used in this test, future tests should be set up to examine effects from different smoothness, duration and complexity of linear motion in conjunction with changes in sampling rate before exploring other noise reduction techniques.

Cost Justification

Low cost microcontrollers such as the AVR architecture processors can cost $1.75 in bulk quantities whereas faster ARM architecture chips cost around $5.50 in bulk. Both chips can achieve 2-3 cycle multiplications for their word size, but the ARM design with average maximum clock speeds of 120 MHz and 32 bit registers can achieve roughly 12 times the computational throughput as the 16 MHz average maximum AVR chips (8 bit registers for a 16 bit number). By decreasing the computational overhead required for processing sensor data by a factor of 15, cost is reduced by a factor of 3. The complexity of sampling faster requires more overhead to the context switch to keep up with the other responsibilities of the processor, so the ultimate complexity of sampling increases at a similar rate. This lowers the sampling rate and aligns the cost more linearly with the computational overhead required.

Discussion of Future Experiments

The primary purpose of applying the different treatments is to find ways to better overcome the noise sources inherent to motion in an inertial reference frame. The main sources of noise are in the experiment used are:

1. High frequency signals due to imperfections in the track rails and wheels in addition to noise introduced by the power supply (~100 Hz).
2. Medium frequency noise due to the mass-spring damper system created by the weight connected by a partly elastic string (~10 Hz).
3. Low frequency noise resulting from the cart wheels ricocheting of the side of the rails due to misalignment (~1 Hz).

This mass-spring damper noise has the largest magnitude of the 3 because it is aligned purely with the axis of motion. The friction of the string on the end of the rail is small and the resulting system is underdamped so these oscillations exist for some time during the positive acceleration portion of the measurement. It is

expected that these oscillations could be fully integrated by the sensors due to their relatively slow frequency and thus do not constitute a problem for the sensors. The low frequency noise due to the misalignment cannot be corrected by any of the methods currently used in the experiment and require sensor fusion with a gyroscope and statistical filtering techniques such as the Kalman filter to eliminate them.
The first noise source is the primary target of the methods used in this experiment. Since they are on the same order of the sampling rate, a significant portion of the high frequency signals will occur above the Nyquist frequency, resulting in aliasing effects and random error offsets dependent on the magnitude of the noise. It was expected that the low pass filtering would help reduce the uncertainty introduced to the integration by these high frequency signals but the results indicate that this can only be accomplished with an increase in the sampling rate. One likely explanation for this is that digital filtering of the already aliased signal cannot reduce the bias offset because it has been irreversibly added to the system. Therefore the intuition that led to the hypothesis in the first place may still be valid in the case that low pass filtering is applied before the analog to digital conversion in hardware.

Future experiments should explore the application of sensor fusion for controlled movements. It was discovered in this experiments conducted prior to this one that drift due to simple sensor fusion algorithms dominate the overall error in position. The best use of resources would be to first try to get accurate results from an improved algorithm such as the Kalman Filter which takes into account knowledge of the variance of the sensor measurements to make an estimate of position that can be weighted with its probability of being seen only due to noise effects before being integrated. Using these methods it is expected the relative error can be centered on zero, and then further improvements in faster sampling accelerometers and gyros with hardware filtering can be used to improve the variance of position estimates up to a limit defined by noise due the power supply and the physical accuracy of the sensors.